Effect of Chemical Structure and Shear Force on the Morphology and Properties of Jet Printed Black Micropatterns Using Imide Epoxy Binders

Chi-Jung Chang, Meng-Wei Wu, Chia-Ming Wu

Department of Chemical Engineering, Feng Chia University, Seatwen, Taichung, Taiwan 40724, Republic of China

Received 11 April 2008; accepted 20 May 2008
DOI 10.1002/app.28978
Published online 30 October 2008 in Wiley InterScience (www.interscience.wiley.com).

ABSTRACT: Epoxy and epoxy acrylates with phthalimide groups on the main chain or pendent side chain were synthesized and used as binders for solvent-free UV-curable inks. Effects of chemical structures on the solubilities of binders in monomers, together with the influences of shear force and ink compositions on the morphology and nanoindentation properties of the microstripes were studied. PIK1 inks containing BAPSBD epoxy with phthalimide groups on the main chain showed shear-thinning behaviors and pigment aggregation problems. Variations of the shear stress at different positions of the dispenser led to PIK1 microstripes with rough central regions and smoother edges. AMPDP acrylate with pendent phthalimide side chain afforded not only good solubility in monomers but also good thermal and mechanical properties after curing. Stripes prepared by the PIK2 ink containing AMPDP exhibited straight edge and smooth surface. Considering the solubility and compatibility in inks, together with properties of cured stripe, binders with pendent phthalimide groups are better candidate as UV-curable ink compositions than those with main chain phthalimide groups. © 2008 Wiley Periodicals, Inc. J Appl Polym Sci 111: 1391–1399, 2009

Key words: morphology; compatibility; dispersion; nanoindentation

INTRODUCTION

Polymer-particle dispersions find applications in a growing number of products, including paints, inks, cosmetics, and pharmaceutical formulations.[1,2] Flow behavior of dispersions is very important in these applications. Shear force caused by spin-coating and rubbing can change the morphology of the thin film. Shear alignment of liquid crystal and block copolymers have been studied. Varghese et al.[3] investigated the planar alignment of liquid crystals, which is enforced with specific polyimide layers and mechanical rubbing procedure. Angelescu et al.[4] reported the formation of dot-array templates with excellent long-range order by applying shear force on the thin films of block copolymers.

Color filter consists of black matrix (BM) and color pixels. BM stripes are arranged between RGB (red, green, and blue) color pixels. BM not only increases contrast by suppressing mixing between colors but also prevents the malfunction of thin film transistors (TFT) because of light leaking. Many studies[5,6] have been made on forming BM patterns using a resin BM (photosensitive resin dispersed with light-shielding pigment) by the photolithography process. However, problems such as deterioration of the sensitivity and resolution still need to be improved. The ink jetting processes for manufacturing color filters are developed to replace conventional photolithography process.[7–11] Nakazawa et al.[12] reported a process of manufacturing BM patterns with the ink-receptive layer to prevent ink bleeding between adjacent pixel areas. Other techniques have been developed to make tiny patterns by jet printing and curing of UV-curable inks. UV-curable inks can be water base, solvent base, or solvent-free inks. For the previous two types of inks, the printed inks should be heated to remove water or solvent and then cured by UV light to fix the printed pattern on the glass substrate.[13–15] As shown in Figure 1(a), the barrier rib is necessary to prevent the printed ink from overflowing to the neighboring area during baking. The baking procedure and the preparation of barrier ribs will decrease the throughput of the printed products.

Polyimides exhibit high thermal stability, good solvent resistance, and outstanding mechanical properties.[16,17] However, poor thermoplastic flow properties and bad solubility are major problems for the application of polyimides. Two approaches have been developed for increasing the solubility and processability of polyimides without sacrificing their thermal stability. The first includes the synthesis of imide copolymers such as poly(ester-imide)s,[16–18]

Correspondence to: C.-J. Chang (changcj@fcu.edu.tw).

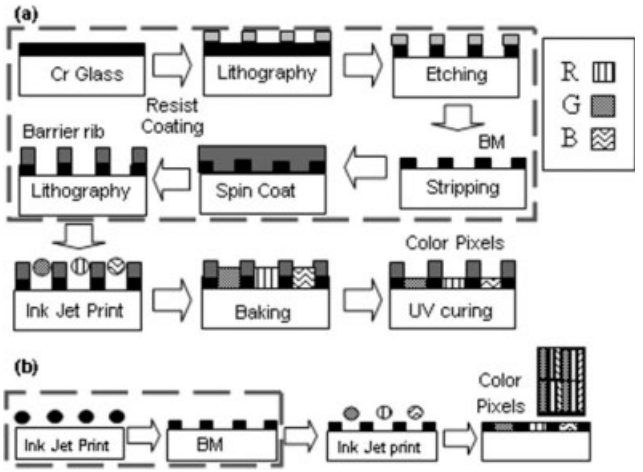

Figure 1 The jet-printed LCD color filter manufacturing procedures prepared by (a) Cr black matrix, barrier ribs, and aqueous UV-curable color inks[15] and (b) nonvolatile UV-curable black and color inks.

poly(siloxane-imide)s,[19–21] and poly(amide-imide)s.[22] The second includes the introduction of flexible linkages[23] and bulky pendant groups along the polymer backbones.[24]

In this article, soluble and thermally stable epoxy and epoxy acrylates with phthalimide groups on the main chain or pendent side chain were synthesized. Feasibility of these materials as compositions of solvent-free UV-curable black inks for jet printed black micropatterns on glass was evaluated. Such ink was the polymer-particle dispersion consisting of monomers, oligomers, initiators, binders, and black pigment. Because there is no volatile solvent, the baking process can be eliminated. After printing the BM patterns, the ink can be fixed immediately by the UV-curing reaction.[25] As shown in Figure 1(b), no receiver layer or barrier rib is necessary to prevent the bleeding problems of the printed micropatterns. During the ejecting of the ink, shear force was applied on the ink by the nozzle. Effects of chemical structures on the solubility of the oligomer in monomers, together with the influences of shear force and ink compositions on the morphology and nanoindentation properties of the microstripes were studied.

EXPERIMENTAL

Materials

Bis[4-(4-aminophenoxy)phenyl]sulfone, acetic anhydride, sodium acetate, DMF, and 1,2,4-benzenetricarboxylic anhydride (BTCA) were supplied by Aldrich. Irgacure 907 (Ciba) and ITX (BASF) were used as received. 2-Acryloxyloxy ethyl phosphate (PA), pentaerythritol triacrylate, (PE-3A), dipentaerythritol hexnacrylate, (PE-6A), and tetrahydrofurfuryl methacrylate were supplied by Kyoeisha. 2,2-Bis[4-(glycidyloxy)phenyl]propane (DGB), 4-amino-*N*-methylphthalimide (AMP), and Bis[4-(4-aminophenoxy)-phenyl] sulfone were purchased from TCI. Black pigment (Clariant) containing 50% carbon black pigment in a vinyl chloride/vinyl acetate copolymer carrier material was incorporated as colorant.

Synthesis of binders and oligomers

4-Amino-*N*-methylphthalimide (AMP) (1.53 g, 8.68 mmol), 2-acryloyloxyethyl phosphate (PA) (0.19 g, 0.96 mmol), and 2,2-bis(4-glycidyloxy phenyl)-propane (DGB) (3.28 g, 9.63 mmol) were dissolved in DMF (15 g). The solution was reacted at 90°C for 8 h to prepare AMPDP polymer. The reaction is illustrated in Scheme 1(a).

As shown in Scheme 1(b), 1,2,4-benzenetricarboxylic anhydride (BTCA) (3.84 g, 20 mmol) was dissolved in DMF (11.52 g). Bis[4-(4-aminophenoxy)-phenyl]sulfone (4.325 g, 10 mmol) was dissolved in DMF (12.975 g) and then added to the BTCA solution. The mixture was stirred at room temperature for 2 h. Acetic anhydride (3.46 g) and sodium acetate (0.24 g) were added. The mixture was heated at 30°C for 1 h, followed by 45°C for 2 h. Then, the reaction mixture was cooled to room temperature, washed with DI water, and filtered. The obtained crude product was washed for five times and dried in vacuum at 90°C for 24 h to afford BAPSB as yellow solid. BAPSB (1 g, 1.2 mmol) and DGB (0.43 g, 1.2 mmol) were dissolved in DMF (4.29 g) and reacted at 150°C for 8 h to prepare BAPSBD polymer. The reaction scheme is shown in Scheme 1(c).

4-Amino-*N*-methylphthalimide (AMP) (1.71 g, 9.7 mmol) and 2,2-bis(4-glycidyloxy phenyl)-propane (DGB) (3.29 g, 9.7 mmol) were dissolved in DMF (15 g). The solution was reacted at 100°C for 7 h to prepare AMPD polymer. The reaction is illustrated in Scheme 1(d).

Ink preparation and pattern formation

Black pigment was dissolved in tetrahydrofurfuryl methacrylate to make the pigment concentrate. AMPDP oligomer (or BAPSBD binder) was dissolved in tetrahydrofurfuryl methacrylate and then mixed with the initiator (Irgacure 907 and ITX), pentaerythritol triacrylate, and dipentaerythritol hexnacrylate. The formulations of the PIK1 and PIK2 inks are listed in Table I. The solution mixture was stirred for 2 h and then slowly added into the pigment concentrate. The solution was stirred for 1 h to make the ink. The black ink was printed on the glass substrate by the dispenser and fixed after UV curing. The internal diameter of the dispensing head is 260 μm. The head moving speed is 40 mm/s.

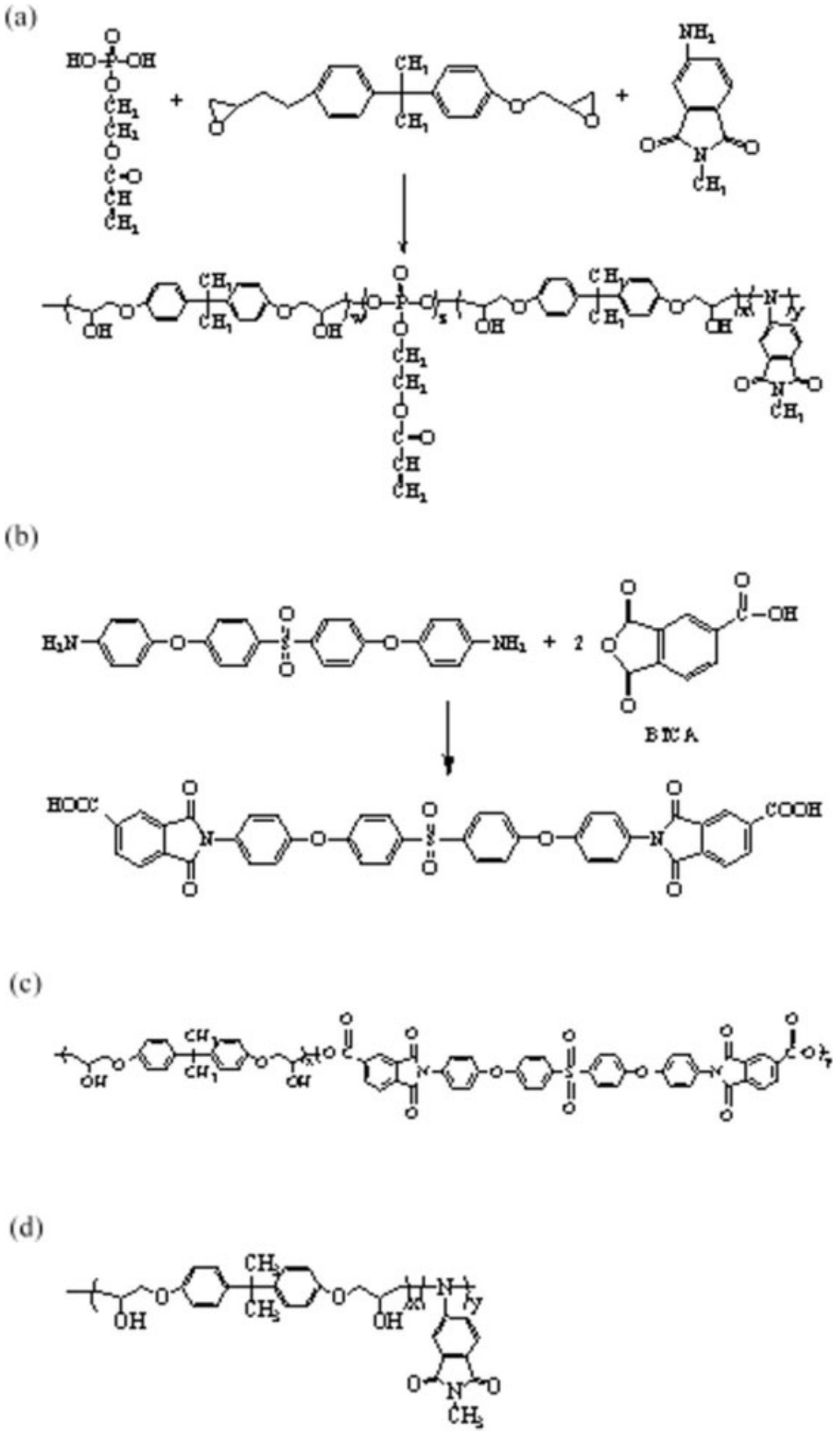

Scheme 1 Reaction schemes of synthesizing (a) AMPDP oligomer and (b) BAPSB and chemical structures of (c) BAPSBD binder and (d) AMPD binder.

Characterization

Thermogravimetric analysis (TGA) was carried out using a TGA2950 apparatus from TA Instruments at a scan rate of 10°C/min under nitrogen atmosphere. The viscosity of the ink was measured using a Brookfield DV III viscometer. SEM measurements were conducted with a HITACHI S3000 Variable Vacuum Scanning Electron Microscope and Energy

TABLE I
Compositions of the PIK1 and PIK2 Inks

Ink composition	PIK1 (wt %)	PIK2 (wt %)
Black pigment	2	2
Tetrahydrofurfuryl methacrylate	21	21
Pentaerythritol triacrylate	13	13
Dipentaerythritol hexaacrylate	60	60
BAPSBD (binder)	2	
AMPDP (oligomer)		2
ITX (photoinitiator)	1	1
Irgacure 907 (photoinitiator)	1	1

dispersive Spectrometer. Two nanoindenters were used in this study. The nanoindentation properties of the neat polymeric films were measured by the Hysitron system to compare the mechanical properties of different binders. The Hysitron system gave high resolution at smaller penetration depths. The nanoindentation test involved indentations with maximum load at 950 μN. On the other hand, the indenter of the MTS system can be precisely placed on a selected tiny area such as the UV-cured stripes. Nanoindentation properties of the stripes were measured by the MTS system with a Berkovich indenter. Loading-unloading cycles are performed at 12 analogous locations on the sample. The normal force (F) is loaded until a maximum indentation depth (d_{max}) of 600 nm is reached. The maximal load is hold during 7 s to minimize the viscoelastic effects of the polymer during the unloading (creep or relaxation). The force is then unloaded. During each cycle, the applied load and the penetration depth are recorded to detect the hardness and modulus of the cured stripe. All experiments have been performed at 22°C ± 2°C.

RESULTS AND DISCUSSION

TGA

The thermal stability and degradation behavior of the phthalimide epoxy binder and UV-cured polymer were evaluated by TGA under nitrogen atmosphere. Figure 2 shows the TGA thermograms of AMPD binder, cured AMPDP, and BAPSBD binder. T_d represents the temperature at 10% weight loss. T_d of the BAPSBD binder consisted of pendent phthalimide side chain is 340°C. T_d of the AMPD binder consisted of pendent phthalimide side chain is 290°C. AMPDP is a UV-curable oligomer prepared by replacing 10% (mole ratio) AMP with phosphoric acrylic segments. Compared with cured AMPDP, the temperatures of rapid weight loss of the AMPD binder sample shifted to higher temperature regions. UV-cured AMPDP had similar T_d as BAPSBD. However, within the rapid weight loss region, the slope of the BAPSBD binder is lower than those of the AMPD binder and cured AMPDP polymer. From the results of T_d and rapid weight loss curve, the BAPSBD binder exhibited better thermal stability than the AMPD binder and cured AMPDP polymer did.

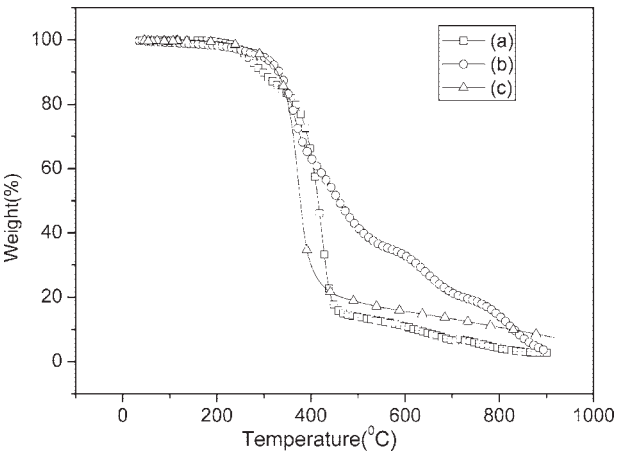

Figure 2 TGA thermograms of (a) AMPD binder, (b) BAPSBD binder, and (c) cured AMPDP.

Nanoindentation properties of binders

Figure 3 illustrates the nanoindentation force-depth curves of the three binders measured by the Hysitron system. The hardness of the AMPD binder, cured AMPDP, and BAPSBD binder (at max load = 1000 μN) were 0.24, 0.22, and 0.28 GPa, respectively. The modulus of the AMPD binder, cured AMPDP, and BAPSBD binder were 7.7, 7.7, and 8.0 GPa, respectively. Differences in the material properties

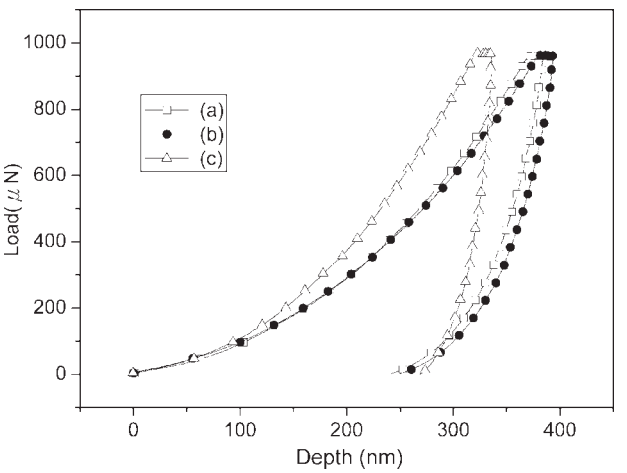

Figure 3 Nanoindentation force-depth plots of thin films prepared by (a) AMPD binder, (b) cured AMPDP, and (c) BAPSBD binder.

TABLE II
Solubility of the Binders in Different Solvent and Monomer

Solvent	Solubility		
	BAPSBD	AMPD	AMPDP
DMF	+ +	+ +	+ +
DMSO	+ +	+ +	+ +
THF	+	+	+ +
Cyclohexane	−	+ +	+ +
Tetrahydrofurfuryl methacrylate	+	+	+ +

Solubility test: 5 mg (binder)/1 g (solvent or monomer).
+ +: soluble at room temp., +: soluble after heating (50°C), −: insoluble.

and time-dependent deformation behavior are interpreted in terms of the chemical structure of the polymers. Both the BAPSBD and AMPD polymers consisted of rigid phthalimide group. However, the locations of the phthalimide groups were different from each other. Phthalimide groups of BAPSBD and AMPD polymer located at the main chain and pendent side chain, respectively. The high hardness and modulus exhibited by AMPD and BAPSBD films indicated that the differences in the phthalimide group location showed little influences on the nanoindentation properties of the films. Both the AMPD and BAPSBD films showed greater resistance to plastic deformation, scratching, and wear as well as resistance to local penetration on application of external force. Although the cured AMPDP is a crosslinked polymer, the aliphatic acryloyloxyethyl side chain increases the free volume of the polymer and leads to lower hardness than the BAPSBD and AMPD films. Results demonstrate that the nanoindentation technique is an effective method of differentiating the mechanical behavior of polymeric materials with different chemical structures.

Solubility

Solubility of the oligomer and binders in different solvent and monomer is listed in Table II. AMPDP was prepared by incorporating 10% of the phosphoric acrylate segments. Crosslinked structure was formed after UV curing. UV-cured AMPDP had similar T_d as BAPSBD. Although cured AMPDP showed similar heat resistance as the BAPSBD binder, AMPDP oligomer exhibited better solubility in many solvent and tetrahydrofurfuryl methacrylate than the BAPSBD binder. Introducing bulky phthalimide pendant groups along the polymer backbones helped to increase the solubility of the AMPDP oligomer. Such an increased solubility is essential to materials used as the jetting ink composition. In this study, patterns were prepared by jetting and curing of nonvolatile UV-curable ink. Such ink is the polymer-particle dispersion consisting of monomers, oligomers, initiators, binders, and black pigment. Because no solvent is added in the ink, oligomers, initiators, and binders must be dissolved in monomers. The pigment must have good compatibility with other compositions. Otherwise, pigment aggregation or binder phase-separation may lead to printing instability or deteriorated printing patterns.

Rheological properties of inks

The rheological property determined the processibility and end-use property of the polymer binder. Figure 4 demonstrates the viscosities of the PIK1 and PIK2 inks measured at different shear rate. The PIK1 ink showed shear thinning behavior. The rheological properties of polymers-pigment particles dispersion were governed by many factors.[26] The viscosity arises from the interactions between the particles and polymers. Factors such as molecular architecture, solid content, particle surface properties, and dispersion medium showed large influences on the rheology of a film. The addition of nonadsorbing (free) polymer can cause several events to occur depending on the chemical structure and concentration of the polymer. Phenomena such as depletion flocculation and depletion restabilization have been reported. When the concentration of free polymer is high enough for intermolecular chain–chain overlap, the induced flocculation begins to occur.[27] In this study, the black pigment was originally dispersed in a vinyl chloride/vinyl acetate copolymer carrier. The viscosity of the PIK1 ink dispersions turned lower at higher shear rates and then reached a stable value. The depletion flocculated network structures were disrupted at high shear rates. However, the

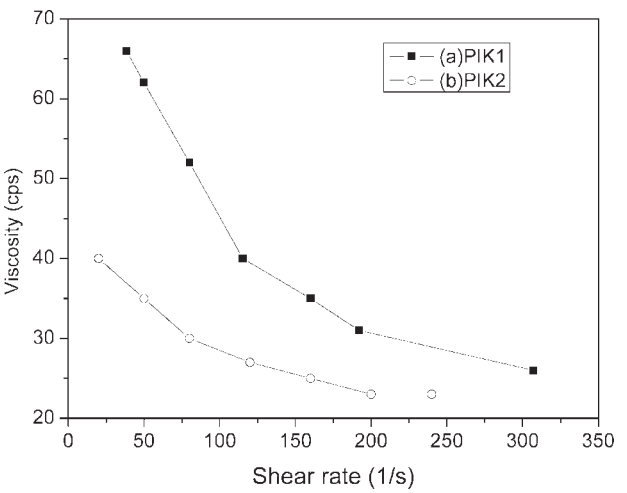

Figure 4 Viscosities of the PIK1 and PIK2 inks measured at different shear rate.

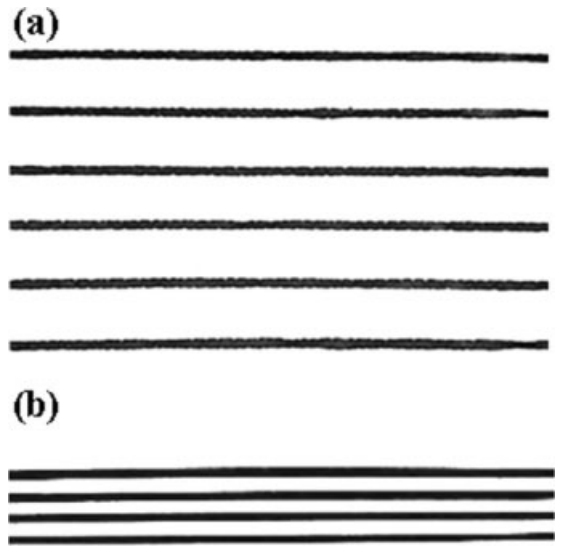

Figure 5 OM images of UV-cured black stripes made by jet printing of (a) PIK1 ink containing BAPSBD binder and (b) PIK2 ink incorporating AMPDP binder on the glass substrates.

influence of increasing the shear rate on the viscosity of PIK2 ink is less than that of the PIK1 ink.

Stripes morphology

The OM image of the printed black stripe made by jet printing of PIK1 ink and PIK2 ink is shown in Figure 5. As shown in Figure 5(a), geometrically irregular bamboo-like surfaces were observed on the stripes prepared by the PIK1 ink. The patterns were similar to the extrudates observed during unstable flow.[28] On the contrary, the PIK2 stripe exhibited straight edges and good color uniformity.

Figure 6(a,b) demonstrates the SEM images of the UV-cured black stripes made by jet printing of PIK1 and PIK2 ink. The morphology of the printed stripe has strong correlations with the ink composition and the shear stress. PIK1 inks containing BAPSBD epoxy with phthalimide groups on the main chain showed shear-thinning behaviors (Fig. 4). Variations of the shear stress acting on the PIK1 ink at different positions of the dispenser led to microstripes with rough central regions and smother edges. The fluid behavior is similar to falling fluid inside the micro-pipe (dispensing tip) with a gas pressure exerting from the top. The shear stress (τ) can be described as follows[29]:

$$\tau = \left(\frac{P_0 - P_L}{2L}\right) r$$

where L, r, P_0, and P_L represent the length of the dispenser, radial position, pressure at the top, and bottom of the dispenser, respectively. The maximum shear force occurs on the pipe wall ($r = R$, radius of the dispenser). The shear stress acting on the fluid decreases as the position moved toward the center of the pipe. The central part of the cured PIK1 stripe

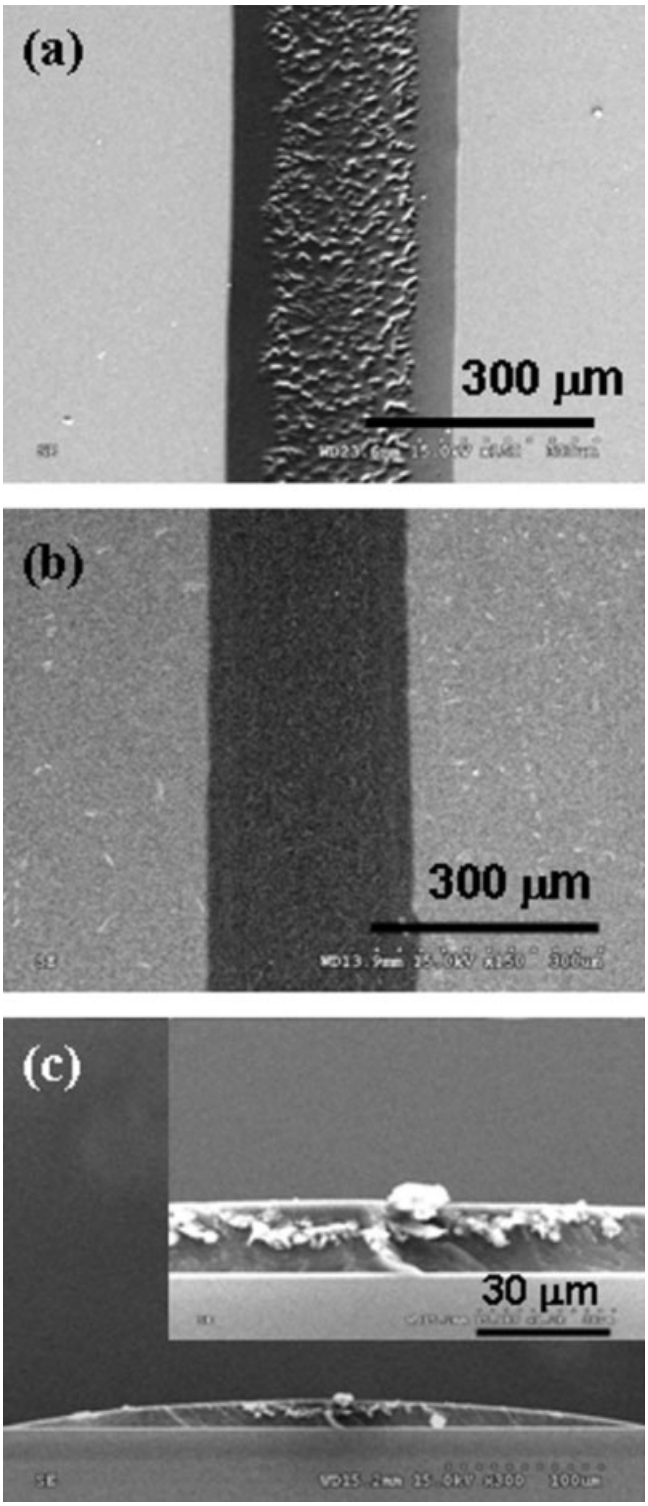

Figure 6 SEM images of the UV-cured black stripes made by jet printing of (a) PIK1 ink, (b) PIK2 ink, and (c) the cross-sectional image of cured PIK2 stripe.

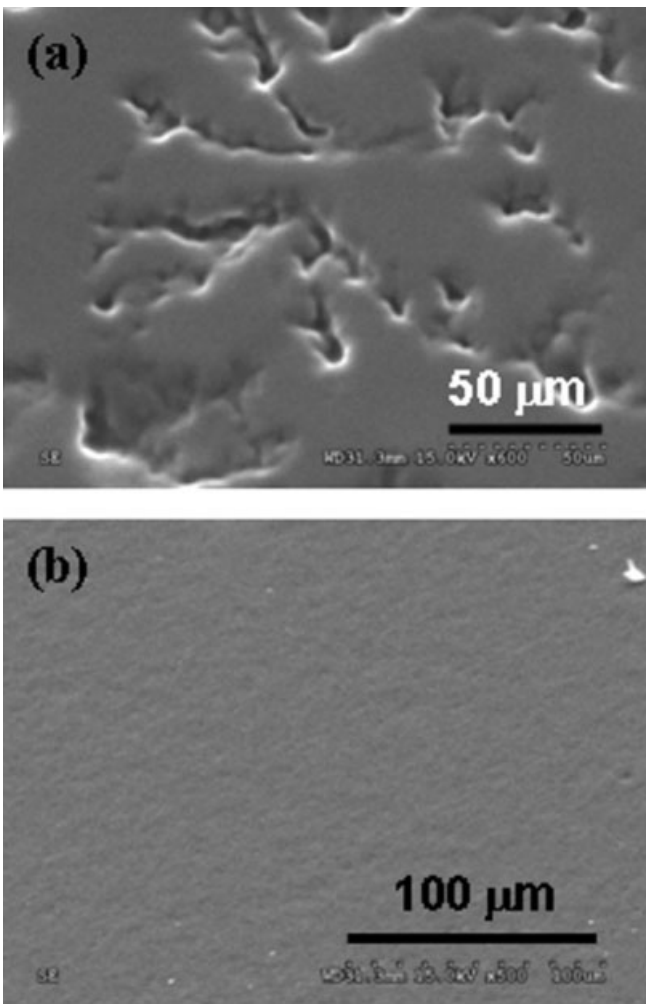

Figure 7 SEM images of the UV-cured black films made by spin coating of PIK1 ink at (a) 1000 rpm (b) 2000 rpm.

showed rough surface, whereas the edge exhibited smother surface. The central parts of stripes mainly consisted of inks near the center of the dispenser pipe. The region near the edge of the stripe consisted mainly of inks near the pipe wall. The rough surface near the central may result from the depletion flocculation. Because the depletion flocculation was disrupted at higher shear rate, the edge of the stripe was smoother than the central part did. During printing, the inks were ejected out of the micropipe with a cylindrical shape. Linear stripes were printed on the glass substrate by moving the dispensing tip. After printing, the printed inks wetted the substrate and slightly flowed before UV curing. The shape and morphology of the stripe were fixed after UV curing. AMPDP acrylate with pendent phthalimide side chain afforded not only good solubility in monomers but also good thermal and mechanical properties after curing. Stripes prepared by the PIK2 ink containing AMPDP exhibited straight edge and smooth surface. Figure 6(c) illustrates the cross section of cured PIK2 stripe. The cross section of the central region is shown in the upper-right corner of Figure 6(c). The thickness of the central region is 16.5 μm.

Figure 7 shows the SEM images of the UV-cured PIK1 films spin-coated at different spin speed. The surface of the film prepared at 1000 rpm [Fig. 7(a)] exhibited rough surface. The cured film [Fig. 7(b)] spin-coated at a higher speed exhibited smoother surface than the lower speed spin-coated one did. Different spin speed resulted in different surface morphology. Shear force had been applied to alter the surface morphology and microstructure of the thin film. Beate et al.[30] reported a significant spin-coating-induced out-of-plane orientation of mesogenic moieties as part of the backbone of LC main chain polyester because of self-organization. In this study, spin-induced shear force changed the surface morphology of the thin film.

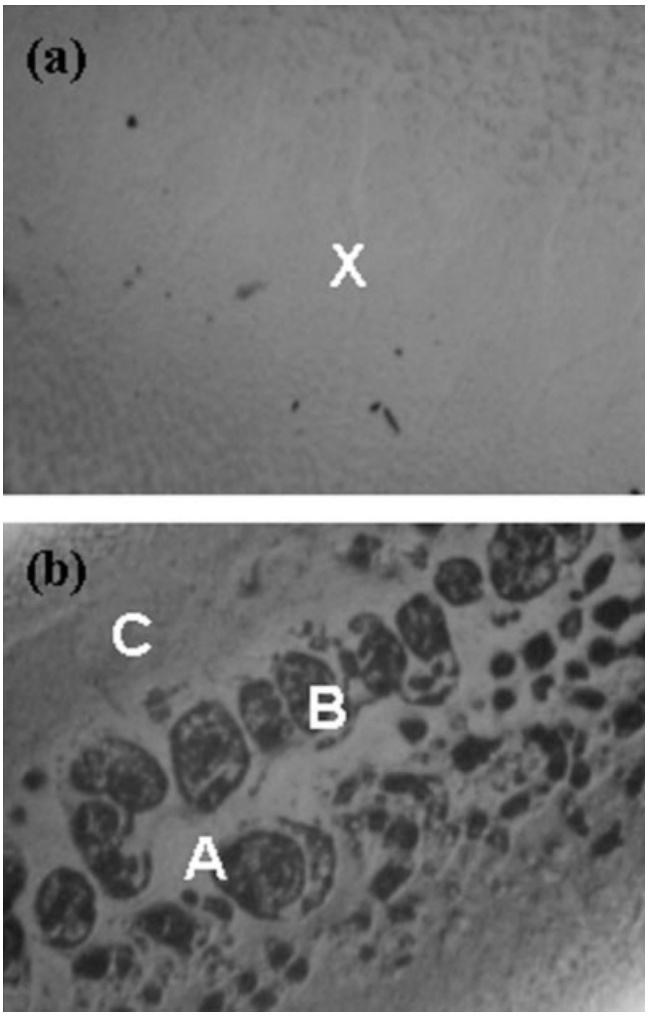

Figure 8 Optical images of the selected areas of cured (a) PIK2 stripes and (b) pigment aggregates (region B), smooth region at the central (region A) and edge (region C) of PIK1 stripes for nanoindentation tests.

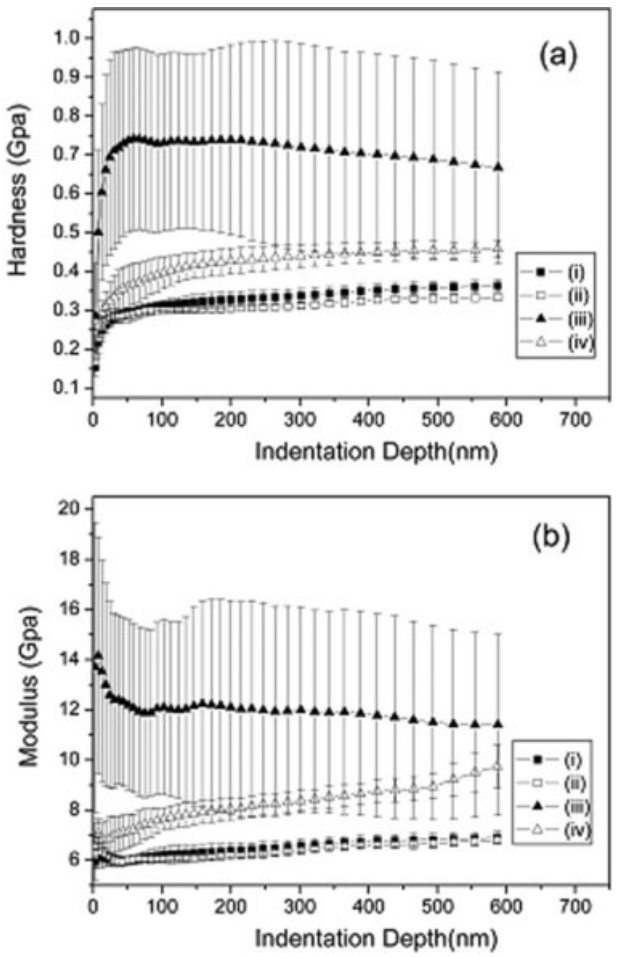

Figure 9 Nanoindentation (a) hardness and (b) modulus of cured (i) PIK2 stripes,(ii) smooth central area (region A), (iii) pigment aggregate area (region B), and (iv) edge area (region C) of cured PIK1 stripes.

Nanoindentation properties of the printed stripes

The nanoindentation tests can be carried out at selected sites of the printed stripes by the MTS system nanoindenter. The hardness and modulus were continuously measured during loading by superimposing a small oscillation on the loading signal and analyzing the system response. As shown in Figure 8, black pigment aggregates (region B) are randomly distributed over the central region of the PIK1 stripes. However, such kind of large aggregates are not found at the edge (region C) of the PIK1 stripes. Because there are phthalimide group on the main chain of BAPSBD, the solubility of BAPSBD in monomers is limited. Adding pigment may further deteriorate the solubility and lead to the aggregate of BAPSBD or pigment. On the contrary, PIK2 stripes exhibited smooth surface morphology. No large pigment aggregate was observed. The nanoindentation properties of the aggregates (region B), smooth region at the central (region A), and edge (region C) areas of PIK1 stripes, together with those of randomly selected sites of PIK2 stripes are shown in Figure 9. The results show a steep increase in hardness at low penetration depths until a plateau is reached for both stripes. The pigment aggregates area showed the highest hardness and modulus than the others did. However, those results of the aggregates area measured at different sites also showed large perturbation. The pigment/binder ratio of the aggregates is higher than that of the smooth region. There are UV-curable compositions in both PIK1 and PIK2 inks. The cured UV-curable compositions and polymer act as binders for the pigments. The large perturbation in the nanoindentation properties of region B (large error bar of curve (iii) in Fig. 9) may result from the differences in pigment/binder ratio among various aggregates. The edge (region C) of the PIK1 stripe showed higher hardness and modulus than the PIK2 stripe and the region A of the PIK1 stripe did. Although the nanoindentation properties of PIK2 stripes are lower than those of PIK1 stripes, PIK2 stripes showed no pigment aggregates. Pigment aggregates deteriorate the color uniformity of the stripes. In addition, the hardness and modulus of PIK2 stripes showed small perturbation. AMPDP with pendent phthalimide side chain showed better compatibility with the pigment and other UV-curable compositions. Considering the morphology, color uniformity, shape, and mechanical properties of the printed stripes, AMPDP is a good candidate as the composition of the nonvolatile UV-curable inks for printing black micropatterns on the glass substrate.

CONCLUSIONS

BAPSBD epoxy and AMPDP acrylates with phthalimide groups on the main chain and pendent side chain were synthesized as solvent-free UV-curable ink compositions for printing black micropatterns. The patterns can be fixed on glass immediately after UV curing. Because no solvent is added in the ink, compositions must be dissolved in monomers. Although BAPSBD showed better thermal and mechanical properties than the cured AMPDP did, PIK1 inks containing BAPSBD epoxy with phthalimide groups on the main chain showed shear-thinning behaviors and pigment aggregation problems. AMPDP showed high solubility in monomer and good compatibility with pigments. Within the dispensing head, the maximum shear force acting on the fluid occurs near the pipe wall. Variations of the shear stress within the dispenser head led to PIK1 microstripes with rough central regions and smother edges. On the contrary, stripes prepared by the PIK2 ink containing AMPDP exhibited straight edge, smooth surface, and good nanoindentation properties. Incorporating bulky phthalimide pendant

groups helped to increase the solubility of the AMPDP oligomer in monomers. Phthalimide groups are introduced to improve the thermal and mechanical properties of the cured stripes. From the viewpoint of solubility and compatibility, this study revealed that binders with pendent phthalimide groups are better than those with main chain phthalimide groups.

References

1. Messersmith, P. B.; Stupp, S. I. J Mater Res 1992, 7, 2599.
2. Huang, X. Y.; Brittain, W. J. Macromolecules 2001, 34, 3255.
3. Varghese, S.; Narayanankutty, S.; Bastiaansen, C. W. M.; Crawford, G. P.; Broer, D. J Adv Mater 2004, 16, 1600.
4. Angelescu, D. E.; Waller, J. H.; Register, R.; Chaikin, P. M. Adv Mater 2005, 17, 1878.
5. Takasaki, R.; Matsuo, F.; Ikeda, S. Jpn. Pat. 2005227797 (2005).
6. Uematsu, Y.; Nomura, S. Jpn. Pat. 2005250179 (2005).
7. Imase, C.; Nishida, T.; Nishiyama, M.; Saito, S.; Sato, K. Eur Pat. 1,266,943 (2002).
8. Hirose, M.; Kashiwazaki, A.; Nakazawa, K.; Shirota, K.; Yamashita, Y.; Yokoyama, M. U.S. Pat. 6,248,482 (2001).
9. Hirose, M.; Kashiwazaki, A.; Nakazawa, K.; Shirota, K.; Yamashita, Y.; Yokoyama, M. U.S. Pat. 6,203,604 (2001).
10. Ewing, P. N.; Holbrook, M.; Kenworthy, M.; Macfaul, P. WO Pat. 200078876 (2000).
11. Kashiwazaki, A. U.S. Pat. 6,475,683 (2002).
12. Nakazawa, K.; Miyazaki, T.; Shirota, K.; Yamada, S. Jpn. Pat. 9,005,730 (1997).
13. Chang, C. J.; Wu, F. M.; Chang, S. J.; Hsu, M. W. Jpn J Appl Phys 2004, 43, 6280.
14. Chang, C. J.; Shih, K. C.; Chang, S. J.; Wu, F. M.; Pan, F. L. J Polym Sci Part B: Polym Phys 2005, 43, 3337.
15. Chang, C. J.; Chang, S. J.; Wu, F. M.; Hsu, M. W.; Chiu, W. W.; Cheng, K. Jpn J Appl Phys 2004, 43, 8227.
16. Mallakpour, S. E.; Hajipour, A. R.; Zamanlou, M. R. J Appl Polym Sci 2002, 85, 315.
17. Chi, Z.; Xu, J. J Appl Polym Sci 2003, 90, 1045.
18. Liaw, D. J.; Fan, C. L.; Lin, C. C.; Wang, K. L. J Appl Polym Sci 2004, 92, 2486.
19. Spontak, R. J.; Williams, M. C. J Appl Polym Sci 1989, 38, 1607.
20. Simionescu, M.; Marcu, M.; Cazacu, M. Eur Polym J 2003, 39, 777.
21. Sysel, P.; Hobzova, R.; Sindela, V.; Brus, J. Polymer 2001, 42, 10079.
22. Banihashemi, A.; Behniafar, H. Polym Int 2003, 52, 1136.
23. Chang, Y. T.; Shu, C. F.; Leu, C. M.; Wei, K. H. J Polym Sci Part A: Polym Chem 2003, 41, 3726.
24. Behniafar, H.; Banihashemi, A. Polym Int 2004, 53, 2020.
25. Chang, C. J.; Tsai, M. H.; Kao, P. C.; Tzeng, H. Y. Thin Solid Films 2008, 516, 5503.
26. Sendijarevic, I.; McHugh, A. J. Macromolecules 2000, 33, 590.
27. Goodwin, J. W.; Hughes, R. W.; Reynolds, P. A.; Kwaambwa, H. M. Colloids Surf A: Physicochem Eng Aspects 2004, 233, 163.
28. Kolnaar, J. W. H.; Keller, A. Polymer 1997, 38, 1817.
29. Bird, R. B.; Stewart, W. E.; Lightfoot, E. N. Transport Phenomena; Wiley: New York, 2002, p 50.
30. Beate, S.; Armelle, B. E. V.; Jürgen, P. R.; Joachim, S.; Götz, W.; Rudolf, Z. Thin Solid Films 2006, 514, 165.